AN INSIGHT ON THE WEAKENING OF THE INTERLAYER BONDS IN A CAMEROONIAN KAOLINITE THROUGH DMSO INTERCALATION

MBEY J. A.[1,2*], THOMAS F.[1], NGALLY SABOUANG C. J.[2], LIBOUM[2] and NJOPWOUO D.[2]

1 Laboratoire Environnement et Minéralurgie, UMR 7569 CNRS-INPL, 15 Avenue du Charmois, B.P. 40. F-54501, Vandoeuvre-lès-Nancy Cedex

2 Laboratoire de Physico-chimie des Matériaux Minéraux, Département de Chimie Inorganique, Université de Yaoundé I, B.P. 812 Yaoundé

MBEY Jean Aimé: jean-aime.mbey@univ-lorraine.fr

NGALLY SABOUANG Cyrill Joël: cngally@yahoo.fr

LIBOUM: liboum2002@yahoo.fr

NJOPWOUO Daniel**:** dnjop@yahoo.fr

THOMAS Fabien: fabien.thomas@univ-lorraine.fr

***** Corresponding author: **e-mail:** jean-aime.mbey@univ-lorraine.fr or mbey25@yahoo.fr**;**

Tel: +237 99 23 89 25

This is the authors version of the article published in *Applied Clay Science:*

An insight on the weakening of the interlayer bonds in a Cameroonian kaolinite through DMSO intercalation
J.A. Mbey, F. Thomas, C.J. Ngally Sabouang, D. Njopwouo
Applied Clay Science 83, 327-335.

http://www.sciencedirect.com/science/article/pii/S0169131713002378

ABSTRACT : In this study, intercalation of dimethylsulphoxide (DMSO) in a cameroonian kaolinite is used to achieve weakening of the interlayer hydrogen bonds, in the perspective of dispersion or even exfoliation of the clay within polymer composite materials. Displacement of intercalated DMSO by ethyl acetate and ammonium acetate is studied in order to simulate the interactions with the polymer matrix. The exfoliation of the kaolinite is well evidenced by X-ray diffraction and SEM observations. The disruption of the interlayer bonds is shown by the displacement of the FT-IR vibration modes of both Al-OH and Si-O functions, and by the decrease of the dehydroxylation temperature recorded by Controlled Rate Thermal Analysis. Complete displacement of DMSO by ethyl acetate is achieved and the crystalline structure is deeply disordered as a result of interlayer bonds weakening. The displacement of DMSO by ammonium acetate leads to a ternary composite of DMSO/ammonium acetate with respective intercalation ratio of 62.4 % and 57.7 %.

***Key words**: Kaolinite, Intercalation, Weakening, Interlayer bond, Composite.*

1. INTRODUCTION

Clays are growingly used in the industry as mineral fillers in polymers composite materials, due to their high aspect ratio and high specific area that determine the intensity of the clay-polymer interactions (Luo and Daniel, 2003). It has been demonstrated for more than two decades that many properties of polymer materials, such as the mechanical or thermal properties, or water and gas barrier effect, can be improved by incorporation of clay particles in the polymer (Arora and Padua, 2010; Pavlidou and Papaspyrides 2008; Ray and Bousmina, 2005; Alexandre and Dubois, 2000).The key factor to achieve such improvements is the dispersion of the clay particles within the polymer matrix. Therefore montmorillonite is most commonly used in polymer-clay composites because of its high surface area and expansible nature of its crystallites which allows complete delamination in aqueous medium (Cabedo et al., 2004).

Kaolinite is widely used in the paper industry as a glossy surface agent in coated papers, diluting agent of titanium dioxide, white pigment, paint extender, or rubber filler (Murray,

2000; Conceicao et al., 2005). Conversely, its use in polymer-clay composites is by far less common (de Carvalho et al., 2001; Whilhem et al., 2003; Chen and Evans, 2005). However, kaolinite is the most ubiquitous clay. Natural kaolinite deposits are sometimes of such purity level that there is not much additional purification required prior to industrial use, since only little contamination with illite/muscovite, quartz, rutile, ilmenite, or feldspar is observed (Murray, 1988). In Africa, the occurrence of kaolinite clay was recently evaluated, and it appears that the exploitation of the occurrences is still to be improved, which offers both investment and research opportunities (Ekosse, 2010). The use of kaolinite as reinforcing filler in the production of polymer-clay (nano)composite is one of the potential applications of interest, and represents the general aim of the present work.

The asymmetrical structure due to the superposition of the tetrahedral and the octahedral sheet in the kaolinite layer induces strong superposed dipoles, which, in conjunction with hydrogen bonds between the silicone oxide ring and the aluminol surface result in strong cohesive energy of the mineral (Cabedo, 2004; Giese, 1988). In addition, the crystalline network of kaolinite is practically devoid of isomorphic substitutions, and does not require charge compensation of hydrated interlayer cations. These characteristics cause kaolinite to occur as non-expandable, large particles of low anisotropy, which explains the lack of interest up to now for its use as mineral filler in polymer-clay composites.

For a convenient use of kaolinite in exfoliated state, one must use a route that ensures weakening of the interlayer bonding between the kaolinite layers, prior to its dispersion within a polymer matrix. There are few organic molecules that can be directly intercalated within the kaolinite. This is the case for dimethylsulfoxide (DMSO), N-methylformamide, acetamide, formamide, potassium acetate; ammonium acetate (Frost et al., 2010; Frost et al., 2003; Itagaki et al., 2001; Frost et al., 1999; Olejnik et al., 1970; Olejnik et al., 1968). These

75 molecules are divided into three types: (i) compounds such as urea or formamide which
76 contain two distinct groups to accept and donate hydrogen; (ii) compounds with a high dipole
77 moment, such as dimethyl-sulfoxyde (DMSO); (iii) ammonium, potassium, rubidium and
78 caesium salts of short-chain fatty acids (acetate, propionate) (Lagaly et al., 2006; Oleijnik et
79 al., 1970). The displacement of the guest molecule from an intercalated kaolinite is often used
80 to promote intercalation of other molecules (Letaief et Detellier, 2007; Cabedo et al., 2004;
81 Itagaki et al., 2001; Komori et al., 1999). Also, the rate at which the displacement takes place
82 is determined by the weakening of the interlayer interactions in the clay. Another interesting
83 factor to consider is the time lasting of the intercalated molecule which, to the knowledge of
84 the authors, was not yet evaluated in the literature, although it is evident that this factor may
85 be of interest in the prospect of the production of a readily usable intermediate product.
86 This paper aims at evaluating the benefit of DMSO intercalation as a pathway toward
87 dispersion of a cameroonian kaolinite to be used within a polymer matrix for composite
88 materials preparation. The rationale is that initial disordering of the kaolinite will determine
89 the dispersion of the particles within the polymer matrix. For this purpose the displacement of
90 the intercalated DMSO by the polymer matrix was simulated in low polarity and ionic
91 medium, respectively ethyl acetate and ammonium acetate, since the polarity of the medium
92 may have consequences on the displacement rate and hence influence the clay structure.
93 X Ray diffraction, infrared spectroscopy and thermal behaviour of the intercalated and raw
94 kaolinite is used as a tool to evaluate the weakening of the layer-layer interactions and
95 stability of the intercalated product.
96

2. MATERIAL AND METHODS

A kaolinite from the Mayouom deposit located at the bottom of a mylonitic cliff in western Cameroon is used in this study. The genesis of this kaolin has been established by Njoya et al., (2006) as a result of a hydrothermal process. This clay has been thoroughly described in the frame of its possible use in ceramic products (Njiomou Djangang et al., 2011; Njoya et al., 2010; Nkoumbou et al., 2009; Djangang et al., 2008; Kamseu et al., 2007).

The sample used in the present study was taken at 3 m depth. The fraction < 40 µm, labelled K3, was collected by means of wet sieving. Using major elemental composition of the sample obtained by inductive coupled plasma by atomic emission spectrometry (ICP-AES), an approximation of the structural formula of the kaolinite phase was found to be $(Al_{1.94}$ $Fe_{0.06})(Si_{1.98}$ $Fe_{0.02})O_5(OH)_4(Mg_{0.02}$ $Ca_{0.002})$. The mineralogical composition of the clay sample, estimated from the chemical composition (table I), the structural formula of the kaolinite phase and from the mineral composition determined by powder X ray diffraction (figure 1), is as follows: Kaolinite 83.3%; Illite 10.4 %; Titanium oxide 3.4 %.

DMSO intercalated kaolinite (labelled K3-D) was prepared using the method described by Gardolinski et al. (2000), excepted that the preparation was performed at room temperature and lasted for 20 days, instead of short stirring at 60 °C followed by a lasting period of 10 days. Typically, 9g of kaolinite were mixed with 60 mL of DMSO and 5.5 mL of demineralised water and left for a 20 days stay. The time-lasting of DMSO intercalation in the clay was tested after 3-years conservation of the dried intercalated samples.

Displacement of the DMSO from the kaolinite was performed using ethyl acetate and ammonium acetate by Prolabo. The respective products are labelled K3-EA and K3-AA. For the K3-AA product, 1 g of K3-D was left to stay at room temperature for 72 hours in 20 mL of a saturated aqueous solution of ammonium acetate. For the K3-AE product, 2 g of K3-D

were heated under stirring at 60 °C in 15 mL of ethyl acetate during 5 minutes and left for a 48 hours stay. For both preparations, the collected clay cake after gravimetric filtration on a 8 µm filter (Whatman grade 40) was left to dry at ambient temperature.

X-Ray powder diffraction patterns were recorded using a D8 Advance Bruker diffractometer equipped with a Co Kα radiation (λ = 1.7890 Å) operating at 35 kV and 45 mA. The diffraction patterns were obtained from 1.5° to 32° at a scanning rate of 1° min^{-1}.

Infrared spectra were recorded in diffuse reflection mode using a Bruker IFS 55 spectrometer. The spectra, recorded from 4000 cm^{-1} to 600 cm^{-1} with a resolution of 4 cm^{-1}, are accumulation of 200 scans.

Scanning Electron Microscopy (SEM) was performed on a Hitachi S-4800 using a YAG (Yttrium Aluminium Garnet) backscatter secondary electron detector for morphological observation on the raw and DMSO-intercalated kaolinite.

Thermal analysis was performed on a home made Control Rate Thermal Analysis (CRTA) apparatus equipped with a mass spectrometer. In CRTA, the temperature increase is not imposed but in controlled by the reaction rate through pressure measurement. The sample is placed under dynamic vacuum through a micro leak that is calibrated so that the emitted gases can be quantified. The limiting pressure is fixed at 2 Pa, which ensures a linear weight loss with time. The emitted gases are analysed by a Balzers (QMS, QMA and QME 200 Pfeiffer Vacuum) mass spectrometer (Feylessoufi et al., 1996).

3. RESULTS AND DISCUSSION

3.1. Intercalation and displacement of the DMSO molecules

The X-ray diffraction patterns (figure 1a) show a complete shift of the characteristic d_{001} peak of kaolinite from 7.19 Å to 11.26 Å. This shift is in accordance with a full monolayer

145 intercalation of DMSO giving rise to a 4.06 Å increase of the basal spacing (Fang et al.,
146 2005).
147 The presence of interlayer DMSO is evidenced on the FT-IR spectrum (figure 2a) by the S=O
148 stretching at 1095 cm^{-1} and by the modification of the external inner surface OH stretching
149 mode at 3693, 3668 and 3651 cm^{-1} (figure 2b) due to interactions of the sulfonyl group in
150 DMSO with the surface Al-OH groups of the clay. The decrease of the band at 3693 cm^{-1} is
151 related to the interaction of the external inner surface hydroxyl with the sulfonyl group in the
152 DMSO molecule. The bands at 3540 cm^{-1} and 3498 cm^{-1} account for the hydrogen bond of the
153 DMSO molecules to some inner surface hydroxyl group of the kaolinite layer (Johnston et al.,
154 1984; Olejnik et al., 1968). The C-S-C symmetric and asymmetric stretching at 659 cm^{-1} and
155 700 cm^{-1} (figure 2a) in the pure liquid DMSO are observable in the intercalated kaolinite at
156 661 cm^{-1} and 719 cm^{-1} (figure 2c).
157 The bending mode of the Al-OH (figure 2 d) is shifted to higher wavelength, due to
158 interaction with DMSO. The Si-O, in plane vibrations at 1020 and 1112 cm^{-1} (figure 2e) are
159 shifted to lower wavelengths. These shifts are evidences for the inner surface oxygen atom
160 interactions with DMSO. Given that, interlayer bonds in kaolinite are due to Al-OH and Si-O
161 interactions, the interactions of these functions with DMSO, necessarily results in weakening
162 of the layer-layer interactions and therefore of the crystallite cohesion.
163 The weakening of the inter-layer interactions is further shown by the dehydroxylation
164 temperature recorded by CRTA (figure 3a and 3b). The dehydroxylation of the kaolinite is
165 completed at 408°C for the raw kaolinite, and at 275 °C for the DMSO-intercalated kaolinite.
166 The changes in pressure are used to detect the dehydroxylation temperature. Mass
167 spectrometry measurements (figure 4a) support this observation. The ion current due to water
168 fragments is plotted as a function of time. The trend of this curves reveal three temperatures

of water release (figure 4a) assigned respectively to hydration water (64 - 90 °C) and to structural water of the kaolinite (408 °C in the raw kaolinite and 273 °C in the DMSO-intercalated kaolinite). The degradation of the intercalated DMSO is observed at 186 °C and the ion currents of both the S=O fragment (m/z = 48) and the CH_3-S-CH_3 fragment (m/z = 62) are consistent (figure 4a) with the degradation of DMSO at 186 °C. The lowering of the dehydroxylation temperature is consistent with lower energy for the interlayer bonds within the clay, in accordance with the conclusion drawn from FT-IR spectra, (figure 2d, and 2g).

The time lasting of the DMSO intercalation in kaolinite was clearly shown by X-ray pattern as well as FTIR spectroscopy that remain unchanged after three years conservation of the sample in a polyethylene bag under ambient temperature. The presented figure 3 and 4 from CRTA as well as the SEM images (figure 6) were obtained using a three years old sample. The comparison with a one month age sample (figure 3b), further confirms the time lasting of DMSO intercalation within the kaolinite. For the one month old sample, the dehydroxylation of the kaolinite is observed at 240 °C. The difference between the dehydroxylation temperatures for the one month and the three year old samples is possibly due to an increase stability of the DMSO-Kaolinite interactions with time as a consequence of the attendant release of co-intercalated water molecules.

Contact with ethyl-acetate leads to almost complete displacement of the DMSO as shown by the disappearance of the peak at 11.26 Å from XRD (figure 1b), which is characteristic of DMSO intercalation. This complete displacement is also evidenced by the O-H stretching modes (figure 5b), which are almost the same for K3-AE and the raw K3, and by the absence of the S=O stretching due to DMSO at 1099 cm^{-1} (figure 5c). The FT IR spectrum for the K3-AE product does not show the carbonyl vibration mode (figure 5e) and the Al-OH bending returns to 916 cm^{-1} as observed in the raw kaolinite (figure 5f). All these observations

193 indicate that the ethyl acetate is not intercalated. However, the stretching and bending bands
194 of C-H on the FTIR spectrum of K3-AE (figure 5a), indicate traces of remaining DMSO
195 within the kaolinite and this presence is evidenced by mass spectroscopy during CRTA
196 (figure 4c) through the ion current of the fragments m/z = 48 (for S=O) and m/z = 62 (for
197 CH_3-S-CH_3). The fact that ethyl acetate does not replace DMSO is probably due to the low
198 polarity of this molecule (dipole moment 1.88) because high dipole moment is a requirement
199 for intercalation in kaolinite (Lagaly et al., 2006). Hence hydrogen bonds of interest are not
200 formed between this compound and the hydroxyl groups within the kaolinite.
201 The use of ammonium acetate also leads to DMSO displacement as shown by the presence of
202 the characteristic basal peak of kaolinite at 7.15 Å (figure 1b). Unlike ethyl acetate,
203 ammonium acetate partially replaces DMSO between the clay sheets. The partial
204 displacement of DMSO is evidenced by X-ray patterns, since the peak at 11.26 Å due to
205 DMSO intercalation is still observable (figure 1b). Also, the IR vibrations mode of S=O from
206 DMSO at 1095 cm^{-1} are detected on the IR spectrum (Figure 5c). The 14.38 Å XRD peak,
207 although weak, is consistent with that described by Itagaki et al. (2001) and Sugahara et al.
208 (1988) for ammonium acetate intercalated kaolinite. It is then suggested that intercalation of
209 ammonium acetate occur in K3-AA. The FT-IR spectra clearly show the presence of
210 ammonium ions within the clay through the bending mode of NH_4^+ that are observed at 1419
211 cm^{-1} (figure 5b) and the carbonyl stretching mode at 1598 cm^{-1} (Figure 5e). The replacement
212 of DMSO by ammonium acetate is associated to the formation of interactions of greater
213 energy than DMSO interactions with the kaolinite hydroxyl groups and this is well confirmed
214 by the bending modes of Al-OH on figure 5f, where the Al-OH bending mode are moved to
215 higher energy compared to the displacement due to DMSO intercalation.

The ion current due to water release during CRTA (figure 4b), clearly shows that the K3-AE and K3-AA have lower dehydroxylation temperatures as proof of the weakening of interlayer bonds. On figure 4b, three dehydroxylation temperatures (90 °C, 362 °C, 417 °C) for K3-AA and two (90 °C and 392 °C) for K3-AE are observed. The dehydroxylation at 362 °C is associated to the part of kaolinite co-intercalated with ammonium acetate and DMSO and at 417 °C we have the dehydroxylation of the recovered kaolinite due to DMSO displacement. The evidence for the dehydroxylation of kaolinite co-intercalated with ammonium acetate and DMSO, is given by the ion current of the fragment of m/z = 14 (related to nitrogen in ammonium acetate) and the fragment of m/z = 48 (related to S=O from DMSO) (figure 4b). At 392 °C the dehydroxylation of the kaolinite recovered from the displacement of DMSO by ethyl acetate is observed and at 90 °C for both K3-AA and K3-AE, the release of the hydration water is observed. The thermal stability of the kaolinite is decreased by the intercalation. Gabor et al (1995) reported the same conclusion in their study of Hydrazine and potassium acetate intercalated kaolinite. The thermal stability, of the kaolinite phase obtain after DMSO displacement, is significantly different and this is due to the induced disordering upon DMSO displacement.

Because the dehydroxylation of the recovered kaolinite after DMSO displacement with acetate ammonium is higher for the recovered kaolinite using ethyl acetate for DMSO displacement, then, one can conclude that, the kaolinite recovered by DMSO displacement with ammonium acetate is less disordered. This observation suggest a high disordering by displacement with ethyl acetate in comparison to displacement by ammonium acetate. The displacement rate may be the cause of this difference. The thermal treatment in the synthesis protocol for the K3-AE is probably the cause of this high displacement rate.

3.2. Effect of the DMSO intercalation and displacement on the kaolinite structure

The DMSO intercalation does not modify the initial kaolinite structure, since the number of layers per crystallite, determined from the coherent domain thickness after the Scherrer equation, remains constant (table II). The SEM micrographs (figure 6) show the morphological evolution due to intercalation. On this image, one can clearly observe that clay stacks appear to be thinner in the intercalated kaolinite than in the raw clay. The intercalation of the kaolinite is evidenced and the conservation of the layer ordering is also observable.

The subsequent displacement of DMSO, strongly affects the kaolinite crystalline structure as shown by the broadening and almost vanishing of the d_{001} peaks on the X-ray patterns (figure 1b). The displacement using ethyl acetate dramatically disorders the kaolinite crystallites. Heller-Kallai and al. (1991) also reported crystallinity reduction in kaolinite samples after DMSO displacement by heating or washing in water. In this study, the drastic change in the crystallinity is probably due to the displacement rate which induce an important disordering particularly for the K3-AE product.

The calculated thickness of the coherent domain in K3-EA shows an increase compared to the pristine kaolinite (from 169 Å to 451 Å) (table II) given a number of layers per crystallite twice as much as in the raw kaolinite (from 25 to 62). In addition, the basal distance for the d_{001} peak is substantially different from that of the pristine kaolinite (7.29 Å in K3-EA against 7.19 Å in the raw material). The explanation of these differences is that high disordering takes place which result in a value for the coherent domain thickness which is not associated to the number of layer per crystallite but rather evidenced the random orientation of clay sheet upon DMSO displacement. Consequently, the number of sheets per crystallite calculated is aberrant. The displacement of DMSO using ethyl acetate does not allow the clay sheets to fall down following a path close or identical to the DMSO intercalation path. In the case of

ammonium acetate, the return path of the clay sheets is almost identical to the initial route of DMSO intercalation. The number of layer in kaolinite pseudo-crystal after DMSO displacement is 25 layers per crystallite (against 24 in the raw kaolinite) and the basal distance is 7.15 Å (7.19 in the raw kaolinite). All of which indicates that the kaolinite phase recovered after the DMSO displacement is structurally very close to initial kaolinite. The dehydroxylation temperature from CRTA also supports this conclusion.

The ammonium acetate intercalation gives rise to a ternary composite and makes it evident that the DMSO displacement is a route for composite preparation. The intercalation ratios (or degree of reaction) within this ternary composite was calculated using the equation below. One must keeps in mind that this equation does not consider the influence of lorentz and polarization factors, the interstratification and layer shape (distortion for example). Hence the relationship is used, assuming, for both expanded and unexpanded phase, the same degree of particles orientation (Lagaly et al., 2006 ;Wang et Zhao, 2006; Olejnik et al.,1968).

$$I.R = I_{001intercalate} / (I_{001intercalate} + I_{001Kaolinite})$$

where $I_{001intercalate}$ is the d_{001} peak intensity due to intercalation; $I_{001Kaolinite}$ is the residual intensity of kaolinite basal peak in the intercalated product and *I.R* is the intercalation ratio.

The calculated intercalation ratios are 57.7 % and 62.4 % respectively for ammonium acetate and DMSO intercalation. The preparation conditions probably determines the intercalation ratios and one can imagine that setting the preparation conditions, for DMSO displacement, will help designing the desired composite. In addition, the structural differences in the recovered kaolinite after DMSO displacement are due to the displacement rate. Ethyl acetate leads to a rapid displacement of DMSO which contributed to higher disordering in the

recovered kaolinite whereas ammonium acetate displacement is less rapid and allows the sheets to almost return to their initial position. This conclusion is corroborated by the results from CRTA. Hence depending on the purpose, the use of DMSO displacement as a route for composite preparation may either need a rapid or low rate for the displacement of the intercalated molecule. In particular, for clay dispersion in a polymer matrix, a rapid and efficient displacement may be needed.

4. CONCLUSION

This study shows the weakening effect of DMSO intercalation in kaolinite and point out the benefits that could be derived from DMSO displacement as a pathway for composite making. The evidence of the intercalation is clearly observed on X-ray patterns and FT-IR spectra. The interlayer interactions are weakened, as revealed by the IR bending modes of Al-OH and the in plane vibrations of Si-O in the kaolinite. This is further confirmed by the dehydroxylation temperature observed in CRTA. The DMSO intercalation is a time lasting modification of the kaolinite. The total displacement of the intercalated DMSO is achieved in hot ethyl acetate medium leading to a random orientation of the clay sheets in the recovered kaolinite due to a great disturbance of the clay sheets interactions. The disordered kaolinite obtained is a consequence of a rapid displacement of the intercalated DMSO. Displacement of DMSO by ammonium actetate follows a path which is similar to that of DMSO intercalation, and a ternatry composite, ammmonium acetate/DMSO/kaolinite is formed.

Hence, if conevenient and adapted conditions are set, the displacement of DMSO from DMSO intercalated kaolinite could be used as a route for composite preparation. In particular, for polymer-clay composite, a rapid displacement may help to obtain optimal dispersion and distribution of the kaolinite as filler within the polymer matrix. The present conclusions have served as basis for the preparation of cassava starch-kaolinite composite films. The

evaluation of the films properties changes confirms that the use of DMSO-intercalated kaolinite is advantageous and the results are subject of a companion paper (Mbey et al., 2012).

Acknowledgement

University of Yaounde I (Cameroon) for laboratory facilities for the synthesis of the kaolinite derivatives.

INPL Nancy (France) for a Doctorate research grant.

References

Alexandre M. and Dubois P. (2000). Polymer-layered silicate nanocomposites: preparation, properties and uses of a new class of materials. *Materials Science and Engineering R,* 28 ,1-63.

Arora A. and Padua G.W. (2010). Review: nanocomposites in food packaging. *Journal of Food Science,* 75 (1), R43-R49.

Cabedo L., Giménez E., Lagaron J. M., Gavara R. and Saura J. J. (2004). Development of EVOH-kaolinite nanocomposites. *Polymer,* 45, 5233–5238.

Chen B. and Evans J. R. G. (2005). Thermoplastic starch–clay nanocomposites and their characteristics, *Carbohydrate Polymers,* 61, 455- 463.

Conceição S., Santos N. F., Velhoc J. and Ferreira J.M.F. (2005). Properties of paper coated with kaolin: The influence of the rheological modifier. *Applied Clay Science,* 30, 165– 173

De Carvalho A. J. F., Curvelo A. A. S. and Agnelli J. A. M., (2001). A first insight on composites of thermoplastic starch and Kaolin. *Carbohydrate Polymers*. 45, 189-194.

Djangang C. N., Elimbi A., Melo U. C, Lecomte G. L., Nkoumbou C., Soro J., Yvon J, Blanchart P. and Njopwouo D. (2008). Refractory ceramics from clays of Mayouom and Mvan in Cameroon . *Applied Clay Science*, 39, 10–18.

Ekosse G-I. (2010). Kaolin deposits and occurrences in Africa: Geology, mineralogy and utilization. *Applied Clay Science,* 50, 212-236.

Fang Q., Huang S., and Wang W. (2005). Intercalation of dimethyl sulphoxide in kaolinite: Molecular dynamics simulation study. *Chemical Physics Letters,* 411, 233-237.

Feylessoufi A., Villiérias F., Michot L. J., De Donato P., Case J.M. and Richard P. (1996). Water Environment and Nanostructural Network in a Reactive Powder Concrete. *Cement and Concrete Composite*, 18, 23-29.

342 Frost R. L., Kristóf J., Paroz G. N. and Kloprogge J. T.(1999). Intercalation of kaolinite with
343 acetamide. *Physics and Chemistry of Minerals*, 26, pp 257-263.
344 Frost R. L., Makó E., Kristóf J., Horváth E. and Cseh T. (2003). The effect of
345 machanochemical activation upon the intercalation of a high-defect kaolinite with
346 formamide. *Journal of colloid Interface Science*, 265, 386-395.
347 Frost R. L., Kristof J. and Horvath E. (2010). Vibrational spectroscopy of intercalated
348 kaolinites. Part I. *Applied Spectroscopy Reviews*, 45(2),130-147.
349 Gábor M., Tóth M., Kristóf J. and Komáromi-Hiller G. (1995). Thermal and decomposition of
350 intercalated kaolinite. *Clays and Clay minerals*, 43 (2), 223-228.
351 Gardolinski J. E., Carrera L. C. M. and Wypych F. (2000). Layered polymer-kaolinite
352 nanocomposites. *Journal of Materials Science,* 35, 3113 – 3119.
353 Giese R. F. (1988). Kaolin Minerals: Structures and Stabilities. In *Hydrous Phyllosilicates*, pp
354 29-66, ed. S.W. Bailey, Mineralogical Society of America.
355 Heller-Kallai L., Huard E. and Prost R. (1991). Disorder Induced by de-intercalation of
356 DMSO from kaolinite. *Clays Minerals*, 26, 245-253.
357 Itagaki T., Komori Y., Sugahara Y. and Kuroda K. (2001). Synthesis of a kaolinite–poly(β-
358 alanine) intercalation compound. *Journal of Materials Chemistry,* 11, 3291 – 3295.
359 Johnston C. T., Sposito G. Bocian D. F. and Birge R. R. (1984). Vibrational spectroscopic
360 study of the interlamellar kaolinite-dimethyl sulfoxide complex. *Journal of Physical*
361 *Chemistry*, 88 (24), 5959-5964.
362 Kamseu E., Leonelli C., Boccaccini D. N., Veronesi P., Miselli P., Giancarlo Pellacani , and
363 Chinje Melo U. (2007). Characterisation of porcelain compositions using two china clays
364 from Cameroon. *Ceramics International*, 33, 851–857.

365 Komori Y., Sugahara Y. and Kuroda K. (1999). Direct intercalation of poly(vinylpyrrolidone)
366 into kaolinite by a refined guest displacement method. *Chemistry of Materials*, 11, 3-6.
367 Lagaly G., Ogawa M. and Dékány I. (2006). Clay Mineral organic interactions. In *Handbook*
368 *of Clay Science*, 1, 309–377, Edited by F. Bergaya, B. K.G Theng and G. Lagaly.
369 Letaief S. and Detellier C. (2007). Nanohybrid materials from the intercalation of
370 imidazolium ionic liquids in kaolinites, *Journal of Materials Chemistry*, 17, 1476–1484.
371 Luo J.-J. and Daniel I. M. (2003). Characterization and modeling of mechanical behavior of
372 polymer/clay nanocomposites. *Composites Science and Technology*, 63, 1607–1616
373 Murray H. H. (1988). Kaolin Minerals: their genesis and occurrences. In *Hydrous*
374 *Phyllosilicates*, pp 67-89, ed. S.W. Bailey, Mineralogical Society of America.
375 Murray H. H. (2000). Traditional and new applications of kaolin, smectite, and palygorskite: a
376 general overview. *Applied clay Science*, 17, 207-221.
377 Mbey J. A., Hoppe S. and Thomas F. (2012). Cassava-starch kaolinite composite film. Effect
378 of clay content and clay modification on film properties. *Carbohydrate polymers*, 88(1),
379 213-222.
380 Njoya A., Nkoumbou C., Grosbois C., Njopwouo D., Njoya D., Courtin-Nomade A., Yvon J.,
381 and Martin F. (2006). Genesis of Mayouom kaolin deposit (western Cameroon). *Applied*
382 *Clay Science*, 32, 125-140.
383 Njoya D., Hajjaji M., Baçaoui A. and Njopwouo D. (2010). Microstructural characterization
384 and influence of manufacturing parameters on technological properties of vitreous ceramic
385 materials. *Materials characterization*, 61, 289–295.
386 Njiomou Djangang C., Kamseu E., Kor Ndikontar M., Lecomte Nana G. L., Soro J., Melo U.
387 C., Elimbi A., Blanchart P. and Njopwouo D. (2011). Sintering behaviour of porous ceramic
388 kaolin-corundum composites: Phase evolution and densification. *Materials Science and*
389 *Engineering A* ,528, 8311– 8318.

390 Nkoumbou C., Njoya A., Njoya D., Grosbois C., Njopwouo D., Yvon J. and Martin F. (2009).
391 Kaolin from Mayouom (Western Cameroon): Industrial suitability evaluation. *Applied Clay*
392 *Science*, 43, 118–124.
393 Olejnik V. S., Posner A. M. and Quirk J. P. (1970). The intercalation of polar organic
394 compound into kaolinite. *Clay Minerals*, 8, 421-434.
395 Olejnik V. S., Aylmore L. A. G., Posner A. M. and Quirk J. P. (1968). Infrared Spectra of
396 Kaolin Mineral-Dimethyl Sulfoxide Complexes. *The Journal of Physical Chemistry* 72 (1),
397 241-249.
398 Pavlidou S. and Papaspyrides C. D (2008). A review on polymer–layered silicate
399 nanocomposites. *Progress in Polymer science*, 33, 1119-1198.
400 Ray S. S. and Bousmina M. (2005). Biodegradable polymers and their layered silicate
401 nanocomposites: In greening the 21st century materials world. *Progress in Materials*
402 *Science* 50, 962–1079
403 Sugahara Y., Satokawa S., Kuroda K., And Kato C. (1988). Evidence for the formation of
404 interlayer Polyacrylonitrile in kaolinite. *Clays and Clay Minerals*, 36(4), 343-348.
405 Wang B. X. and Zhao X. P. (2006). The influence of intercalation rate and degree of
406 substitution on the electrorheological activity of a novel ternary intercalated nanocomposite.
407 *Journal of Solid State Chemistry*, 179, 949-954.
408 Wilhelm H. M., Sierakowski M. R., Souza G. P., and Wypych, F. (2003). The influenced of
409 layered compounds on the properties of starch/layered compounds composites. *Polymer*
410 *International*, 52, 1035-1044.
411

412 Figures and Captions

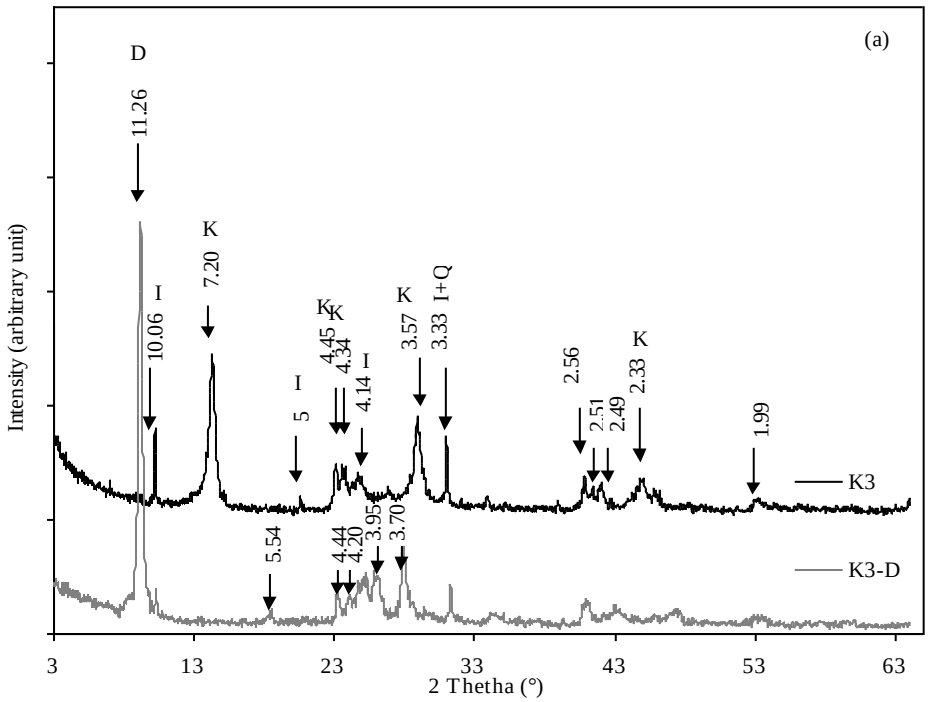

413

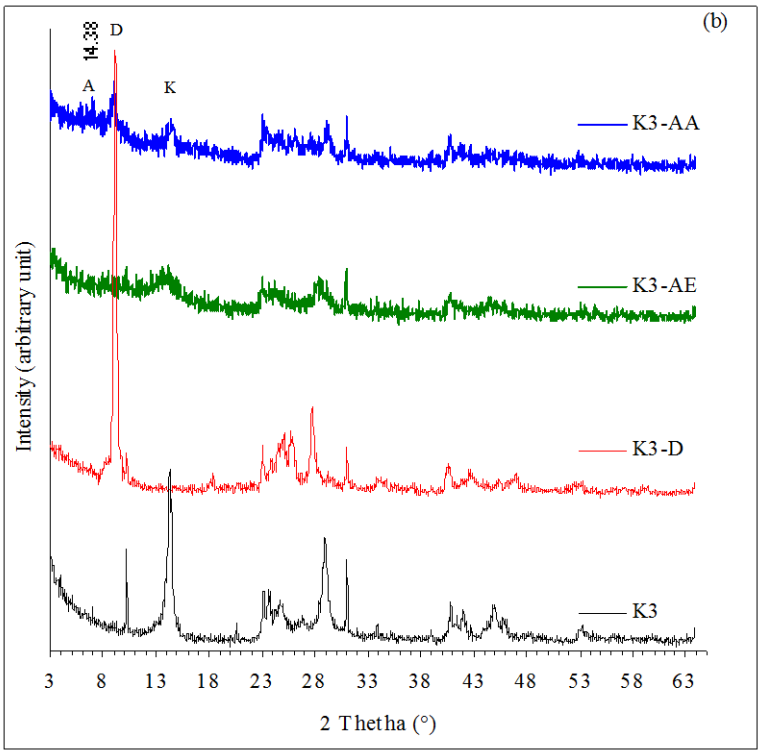

414
415 Figure 1: X-ray patterns of (a) the raw kaolinite and the DMSO-intercalated kaolinite (b)
416 products of MDSO displacement using ammonium acetate (K3-AA) and ethyl acetate (K3-
417 AE).
418 *K : Kaolinite ; I : illite ; D : Kaolinite-DMSO intercalate; A: ammonium acetate-kaolinite*
419
420

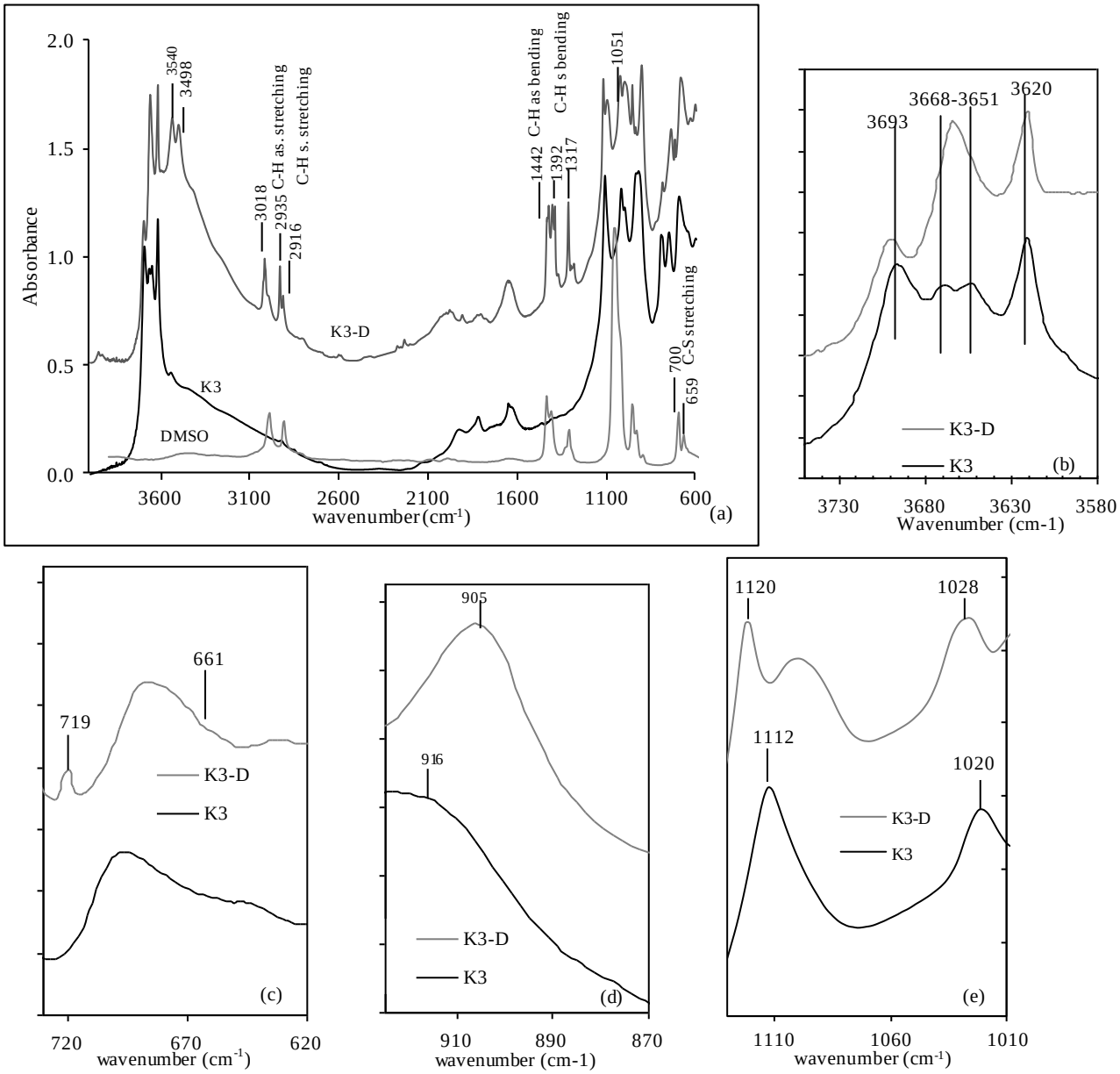

Figure 2: *FTIR spectra: (a) complete spectra of DMSO-intercalated (K3-D), pure DMSO, and raw kaolinite (K3) (b) kaolinite OH stretching band zone (c) stretching of C-S-C bonds of the DMSO molecule (d) bending of the inner surface Al-OH of kaolinite (e) In plane vibrations of Si-O*

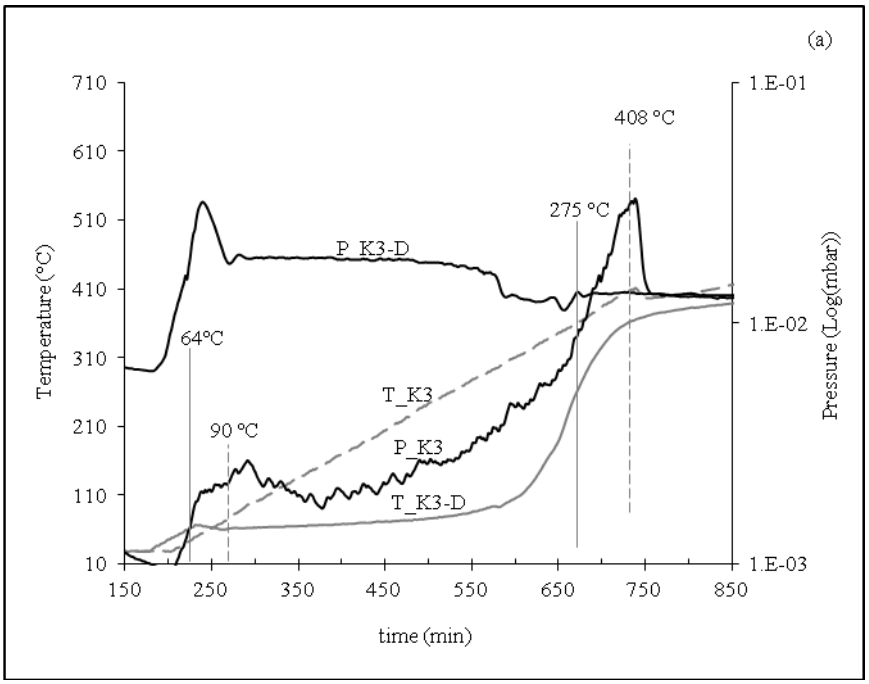

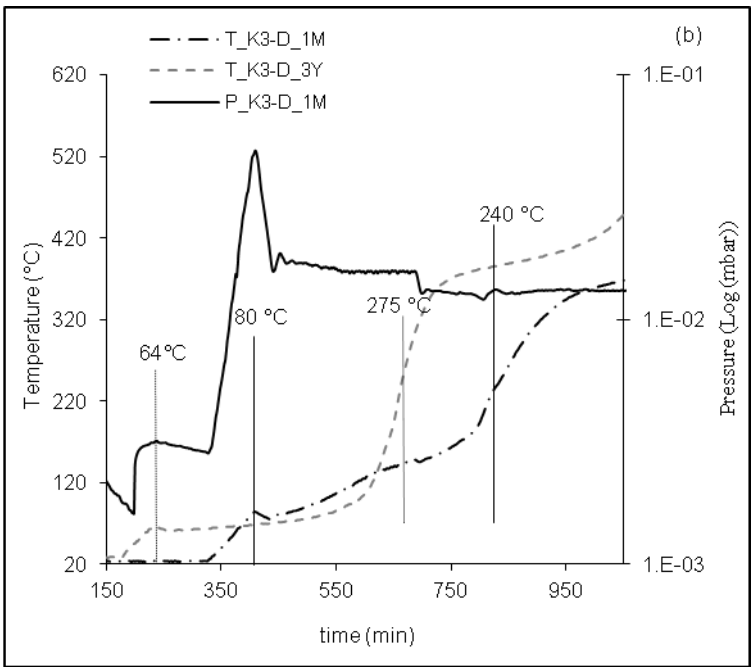

Figure 3: (a) Pressure and temperature evolution during CRTA of the DMSO intercalated (K3-D) and the raw kaolinite (K3) (b) Comparison between a 3 year age (K3-D_3Y) and 1 month age (K3-D_1M) DMSO-Kaolinite.

440

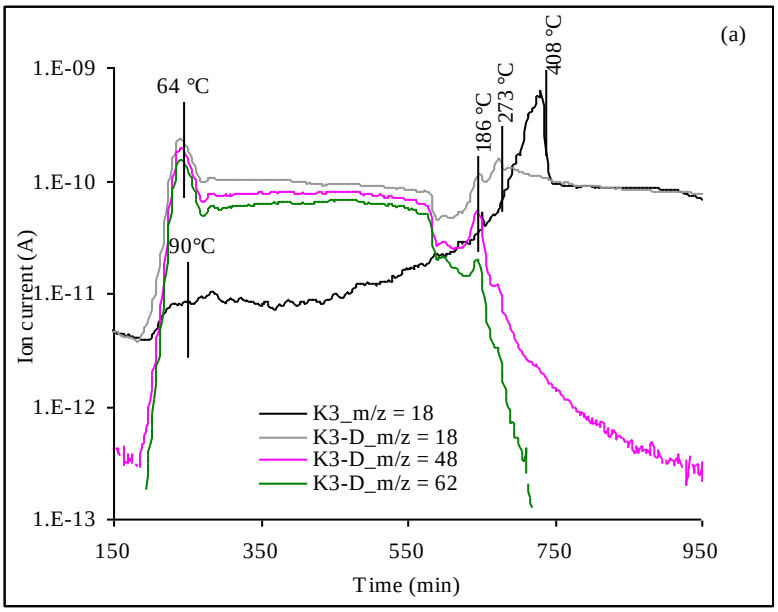

441
442

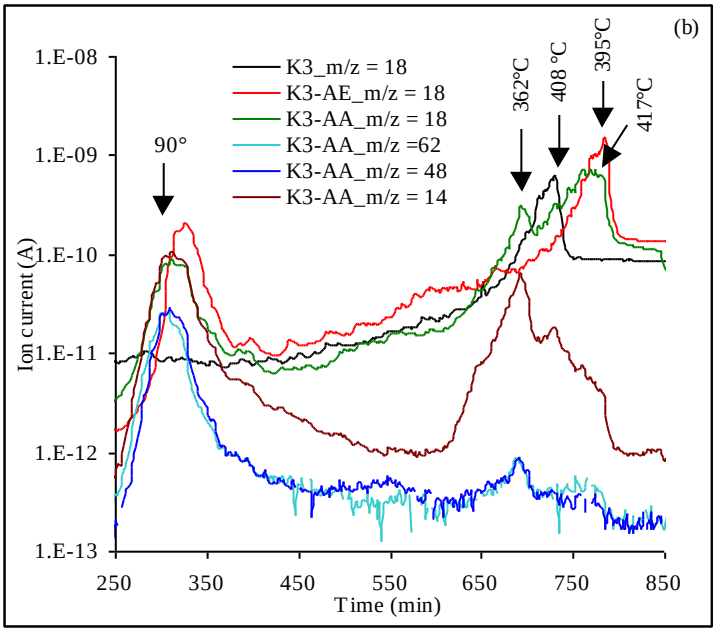

443

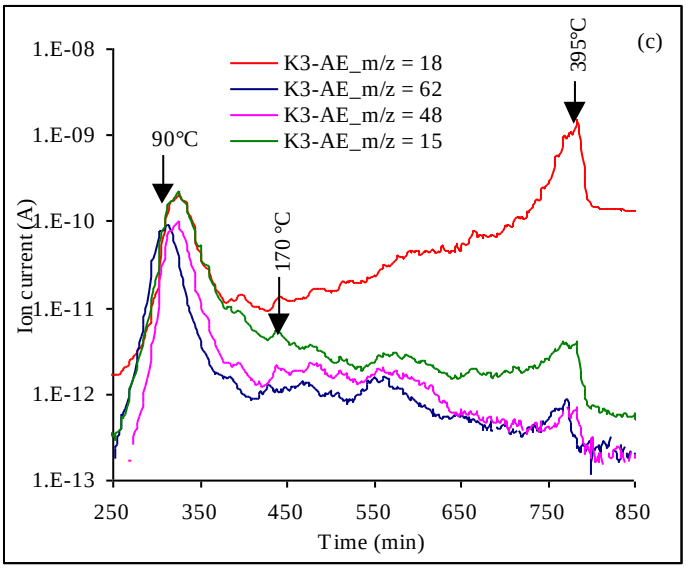

figure 4: Ion current due to water (m/e = 18), S=O (m/e = 48) and CH_3-S-CH_3 (m/e = 62) fragments during thermal treatment of (a) the DMSO-intercalated (K3-D) and the raw kaolinite (K3); (b) products of DMSO displacement using ammonium acetate (K3-AA) and ethyl acetate (K3-AE); (c) Trace DMSO evidence in K3-AE

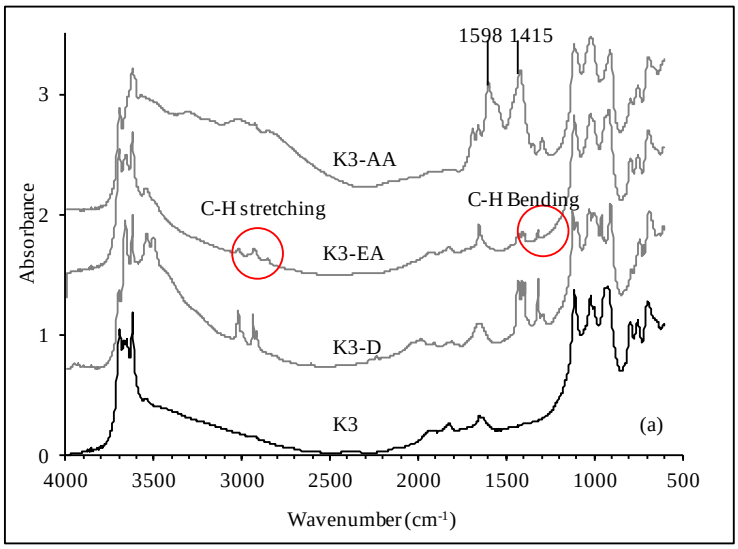
1598 1415
K3-AA
C-H stretching
C-H Bending
K3-EA
K3-D
K3
(a)
Absorbance
Wavenumber (cm-1)

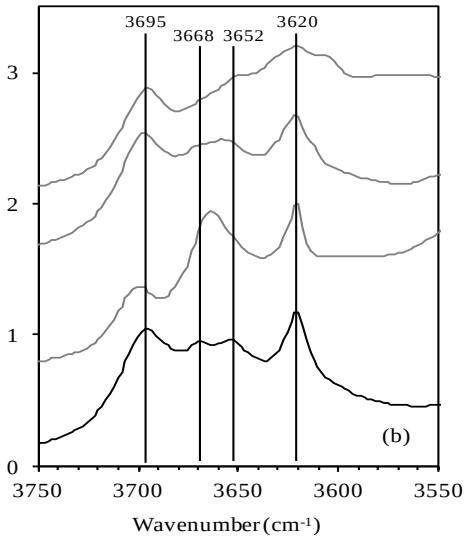
3695
3668 3652
3620
(b)
Wavenumber (cm-1)

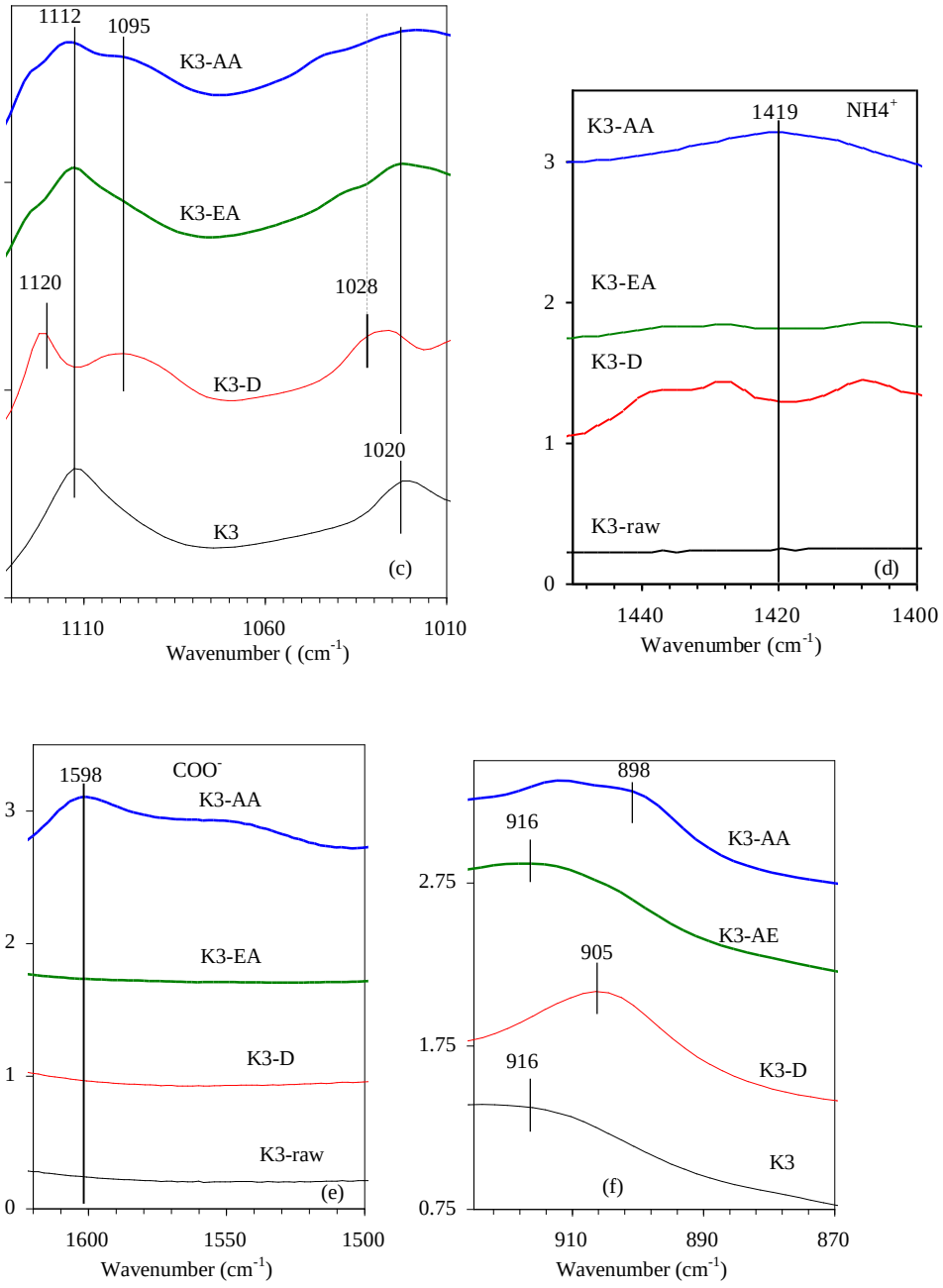

Figure 5: FT-IR spectra of the DMSO displacement in K3 kaolinite using ammonium acetate (K3-D-AA) and ethyl acetate (K3-D-EA): (a) complete spectra (b) O-H stretching domain (c) in plane vibrations modes of Si-O (1112 and 1020 cm^{-1}) and S=O stretching (1099 cm^{-1}). (d) Evidence of $NH4^{+}$ presence (e) Evidence of carbonyl vibration due to COO^{-} group (f) Inner surface Al-OH bending modes.

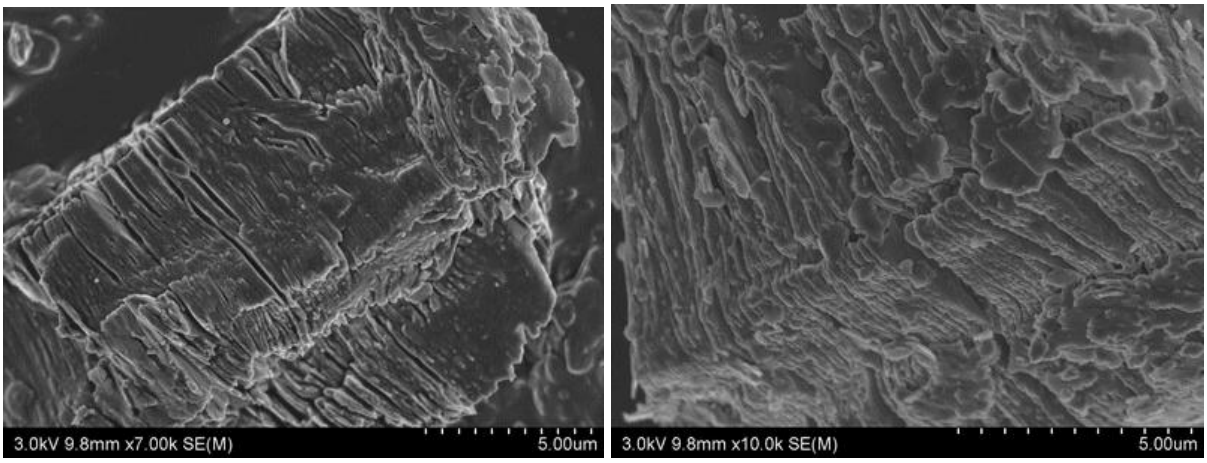

K3 K3-D

Figure 6: SEM micrographs of raw (K3) and DMSO-intercalated (K3-D) kaolinite.